Atomic structures and magnetic behavior of Mn clusters

doi: 10.1103/PhysRevB.66.064412

Atomic structures and magnetic behavior of Mn clusters

Tina M. Briere,[1] Marcel H. F. Sluiter,[1] Vijay Kumar,[1,2,3] and Yoshiyuki Kawazoe[1]
[1]*Institute for Materials Research, Tohoku University, Aoba-ku, Sendai 980-8577, Japan*
[2]*Center for Interdisciplinary Research, Tohoku University, Aoba-ku, Sendai 980-8578, Japan*
[3]*Dr. Vijay Kumar Foundation, 45 Bazaar Street, K. K. Nagar (West), Chennai 600 078, India*
(Received 12 April 2002; revised manuscript received 12 June 2002; published 9 August 2002)

The structures and magnetic properties of Mn clusters containing 13, 15, 19, and 23 atoms have been predicted from *ab initio* electronic structure calculations. The lowest energy structures of the 13-, 19-, and 23-atom clusters are icosahedral and have ordered spin configurations in which blocks of ferromagnetically coupled spins are antiferromagnetically coupled with each other. The 15-atom cluster is body-centered cubic with antiferromagnetic coupling. The net moments are small and lie in the range of $0.2–1.2\mu_B$/atom; however, the average local atomic moments have high values close to $4\mu_B$. These results are discussed in light of recent Stern-Gerlach experiments.

DOI: 10.1103/PhysRevB.66.064412 PACS number(s): 36.40.Cg, 36.40.−c, 61.46.+w, 73.22.−f

The study of the evolution of magnetic behavior from atoms to the bulk is important for the development of magnetic nanomaterials. The occurrence of noncrystallographic structures in small clusters could provide avenues for magnetic phenomena. While several studies have been done[1] on clusters of ferromagnetic materials and the occurrence of magnetism in clusters of nonmagnetic elements, Mn offers a wide range of magnetic properties to excite and challenge theorists and experimentalists alike. The most stable bulk form is α-Mn, with a complicated geometric structure, a low magnetic moment of about $1\mu_B$ per atom, and antiferromagnetic behavior that can be explained by spin waves.[2] However, small clusters (Mn_3-Mn_8) are ferromagnetic, with high moments of $4–5\mu_B$/atom.[3,4] Finally, the dimer is weakly bound, and while recent density functional calculations show ferromagnetic behavior[3–5] there is still some question as to whether the coupling is actually ferromagnetic or antiferromagnetic.[5]

With increasing cluster size, the spin configuration should change from ferromagnetic for small clusters towards bulk behavior, but the intermediate structures are not yet understood. Elucidation of the magnetic behavior in Mn clusters of intermediate size could lead to species with magnetic properties. The $4s^2 3d^5$ configuration of the Mn atom leads to weak bonding and high magnetic moments in small clusters. As the size increases, there should be a delocalization of both the *s* and *d* electrons, leading to metallization of the clusters as well as lowering of the magnetic moments.

A recent Stern-Gerlach experiment by Knickelbein[6] on Mn_{11}-Mn_{99} suggested magnetic behavior that differs from either the bulk or the smaller clusters. Key results include relatively small magnetic moments of $\sim 0.3–1.4\mu_B$/atom with notable local minima at Mn_{13} and Mn_{19} and maxima at Mn_{15} and Mn_{23}-Mn_{25}. The clusters were assumed to be superparamagnetic with ferromagnetic coupling between spins. Icosahedral structures were suggested for the 13- and 19-atom clusters.

With the aim of understanding the above experimental results, we have performed first-principles calculations for clusters containing 13, 15, 19, and 23 atoms. Our results confirm the small net moments per atom observed in experiment as well as icosahedral structures for both Mn_{13} and Mn_{19}. These small net moments arise out of antiferromagnetic or a combination of ferromagnetic and antiferromagnetic couplings between spins in the well-ordered ferrimagnetic clusters. The average local moments on each atom are high, however, with values of about $4\mu_B$.

We used a planewave method employing ultrasoft pseudopotentials[7] and the generalized gradient approximation for the exchange-correlation potential.[8] The $3d$ and $4s$ orbitals were treated as valence states. Clusters were positioned in a cubic supercell with an edge of 15 Å, and periodic boundary conditions were imposed. The cutoff energy for the plane waves was set to 283.9 eV ($\sim$21 Ry), and reciprocal space integrations were carried out at the Γ point. Structural optimizations were performed using quasi-Newton-Raphson and conjugate gradient methods. Structural optimizations were deemed sufficiently converged when the forces were about 1 meV/Å. This level of precision correctly reproduces[9] the ferromagnetic state of the manganese dimer earlier obtained with a similar exchange-correlation functional.

Determination of the low lying spin configurations was a delicate task, as many spin isomers could lie close in energy. We used a variety of methods to find the lowest energy magnetic configurations, including freezing the net magnetic moment of the cluster and specifying the initial magnetic moments on each atom followed by unrestricted optimization. While most initial configurations were ferrimagnetic, some were purely ferromagnetic. Both symmetric and asymmetric spin arrangements were considered. Noncollinear magnetic ordering, however, was not permitted. In all, about 50 geometric and spin combinations were calculated for each cluster size. The local magnetic moments were determined by integrating the spin density over Voronoi cells, which we refer to as ''integrated spin densities'' to avoid confusion with LCAO-type local moments. The thermally averaged net moment was calculated from $\langle \mu \rangle_T = \Sigma_i \mu_i e^{-E_i/k_B T} / \Sigma_i e^{-E_i/k_B T}$, where μ_i is the net moment for isomer i, E_i the total energy, k_B the Boltzmann constant, and T the temperature.

In addition to the icosahedral structures for each cluster size, we also considered decahedral, cuboctahedral, and hexagonal close-packed structures for Mn_{13}, hexagonal and bcc

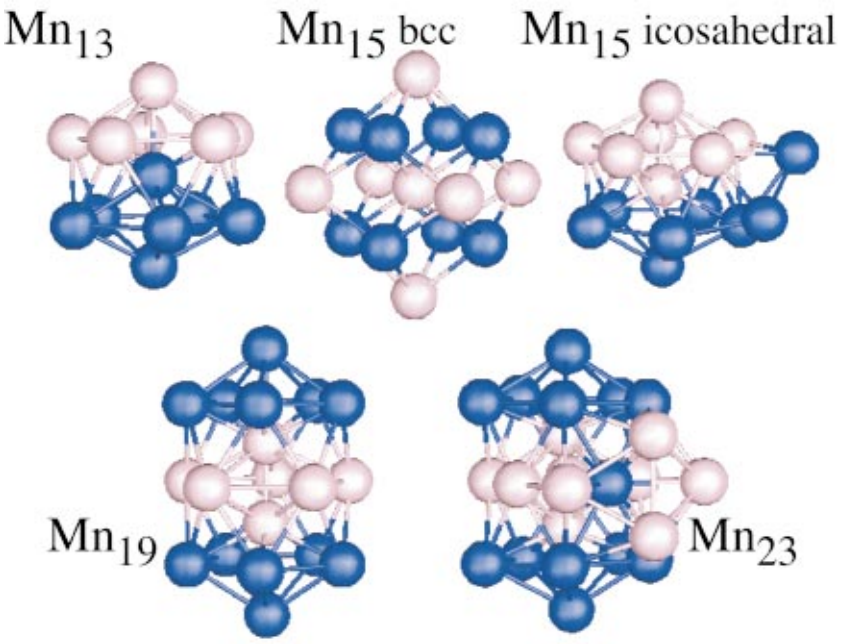

FIG. 1. (Color) Lowest energy structures for each cluster size. Icosahedral Mn_{15} is also shown for comparison. The relative spin alignments are marked, with dark blue indicating spin up and light pink spin down. The local moments, however, have differing values. See the text and Table I for details.

for Mn_{15}, and decahedral and cuboctahedral for Mn_{19}. For Mn_{13}, the decahedral and cuboctahedral structures transformed into icosahedral structures, while the hexagonal close packed structure was a local minimum. Similarly for Mn_{19}, the decahedral structure transformed into a double icosahedron.[10] Figure 1 shows the lowest energy geometry and spin configuration for each cluster size. The icosahedral structures were found to have the lowest energies, except for the case of Mn_{15}, where the bcc was lower than the icosahedral by 0.28 eV. This icosahedral growth sequence for the 13-, 19- and 23-atom clusters has also been seen in clusters of divalent metals such as Ba (Ref. 11) and Sr,[12] which exhibit nonmetal to metal transitions with increasing size. The calculated binding energy increases with increasing cluster size, and has values of 1.84, 1.89, 2.01, and 2.11 eV, for Mn_{13}, Mn_{15}, Mn_{19}, and Mn_{23}, respectively. The maximum value is about 70% of the bulk.

The average bond lengths were calculated by assuming a cutoff of 3 Å. Based on this criterion, the averages for the four cluster sizes vary from 2.62 to 2.65 Å. This is in line with average bond lengths of 2.62–2.73 Å for Mn_3-Mn_8 calculated at the GGA level.[3] For the icosahedral structures, the shortest bond lengths occur for the central atoms bonding between either themselves or with the top and bottom capping atoms (Fig. 1). The shortest bond length for Mn_{13} is 2.41 Å, and for icosahedral Mn_{15} it is 2.36 Å, both longer than the bulk value of 2.24 Å. For bcc Mn_{15}, the shortest bonds (2.41 Å) occur between the central atom and its eight corner neighbors. For Mn_{19} and Mn_{23}, they are respectively 2.25 and 2.29 Å, which is close to the shortest bulk value.

The lowest energy structure of each cluster is ferrimagnetic (Fig. 1). For Mn_{13}, there is ferromagnetic coupling within each five-membered ring as well as between each ring and its nearest neighbor cap. There is, however, antiferromagnetic coupling between the rings. Additionally, the highly coordinated central atom is ferromagnetically coupled with one ring and antiferromagnetically coupled with the other. This leads to a net magnetic moment of only $3\mu_B$. We should note that the low moment is in disagreement with an earlier calculation,[13] in which a moment of $33\mu_B$ was found. However, our binding energy is slightly higher, suggesting that our results show at least a deeper local minimum. Similar spin structures can be seen for Mn_{19} and Mn_{23}, where the spins on the central atoms are antiferromagnetically coupled with those on the upper and lower atoms in the clusters. The ground state structures of these clusters have magnetic moments of 23 and $21\mu_B$, respectively. The lowest energy icosahedral isomer of Mn_{15} also has a spin configuration similar to Mn_{13}. The spins on both of the face capping atoms couple ferromagnetically to one ring and antiferromagnetically to the other (Fig. 1). The net moment is $9\mu_B$. For the bcc isomer Mn_{15}, which is the ground state structure, the spins on the central and face-centered atoms are antiferromagnetically coupled with those on the corners, resulting in a net moment of only $3\mu_B$.

Looking at the results for the icosahedral structures, it appears that ferromagnetic coupling within the five-membered rings is energetically favored, as is fivefold rotational symmetry for Mn_{13} and Mn_{19} and reflection symmetry for Mn_{19} and Mn_{23}. Both high symmetry and ferromagnetic coupling within the five-membered rings cannot be obtained for Mn_{15}, however. Therefore it seems that the more symmetric bcc structure, where nearest neighbor antiferromagnetic interactions result in ferromagnetic planes with antiferromagnetic coupling between, becomes more favorable.

Integrated spin densities are listed in Table I. For all the clusters, the highest coordinated atoms (the central atoms) have the lowest moments, while the surface atoms have the highest. Also, as expected from Pauli repulsion, we find that the ferromagnetically aligned large moments are associated with longer bond lengths than those that are antiferromagnetically aligned. In general the mean value of the integrated

TABLE I. Net magnetic moment per atom and absolute values of the integrated spin densities in μ_B: minimum value, maximum value, and average.

	$\mu_{\text{tot,theory}}$/atom	$\mu_{\text{tot,exp}}$/atom[a]	$\lvert\mu\rvert_{\text{min}}$	$\lvert\mu\rvert_{\text{max}}$	$\lvert\mu\rvert_{\text{ave}}$
Mn_{13}	0.23	0.56±0.13	2.17	4.24	3.91
$Mn_{15,bcc}$	0.20	1.40±0.07	3.22	4.37	4.11
$Mn_{15,ico}$	0.60	1.40±0.07	0.95	4.51	3.81
Mn_{19}	1.21	0.43±0.10	2.19	4.03	3.77
Mn_{23}	0.91	1.23±0.06	0.04	4.35	3.42

[a]Reference 6.

atomic spin densities decreases with increasing cluster size. The exception is bcc Mn_{15}, where the geometrical structure and spin configurations are quite different from the icosahedral clusters. The increase in the average spin density in this case is due to the lower coordination of atoms in the bcc structure. The trend of a decrease in the magnetic moment per atom with increasing cluster size is also in agreement with results from calculations on the smaller ferromagnetic clusters Mn_2-Mn_8 (Ref. 3) as well as the small moment of $\sim 1\mu_B$/atom in the bulk.

Examination of the total density of states (DOS) for the lowest energy structure of each system (Fig. 2) points to the relative stabilities of the different sized clusters. While none of the lowest energy clusters shows a minimum in the DOS at the Fermi energy, the curvatures are all positive. This indicates that each of the clusters is stable with respect to small perturbations in geometry and magnetic configuration. For the smaller clusters, the curvatures in the DOS are relatively large. The corresponding differences between the lowest and second lowest energy spin structures are 0.15 and 0.13 eV, respectively, for Mn_{13} and Mn_{15}. Mn_{19} and Mn_{23} have smaller curvatures in their DOS, suggesting that less energy would be required for excitation to another spin state. This is seen in the small energy differences (0.06 and 0.05 eV, respectively) between spin isomers.

Projection of the local density of states (LDOS) into its *s*, *p*, and *d* components produces interesting site-dependent results. The central, lower ring, and lower atoms in the lowest energy Mn_{13} isomer are shown as an example in Fig. 3. We should note that the *s* and *p* components are significantly underrepresented due to expansion of the wave function into angular momentum components in an atomic sphere with a radius of 1.3 Å. However, the *d*-projected LDOS are of greatest interest here, and our method represents the gross trends properly. The *d*-projected LDOS for the lower ring and lower atoms are similar in that for each the peaks of the LDOS are rather localized and the majority spin is nearly fully occupied. The LDOS is quite low below the Fermi energy for the minority spin. This is in agreement with the

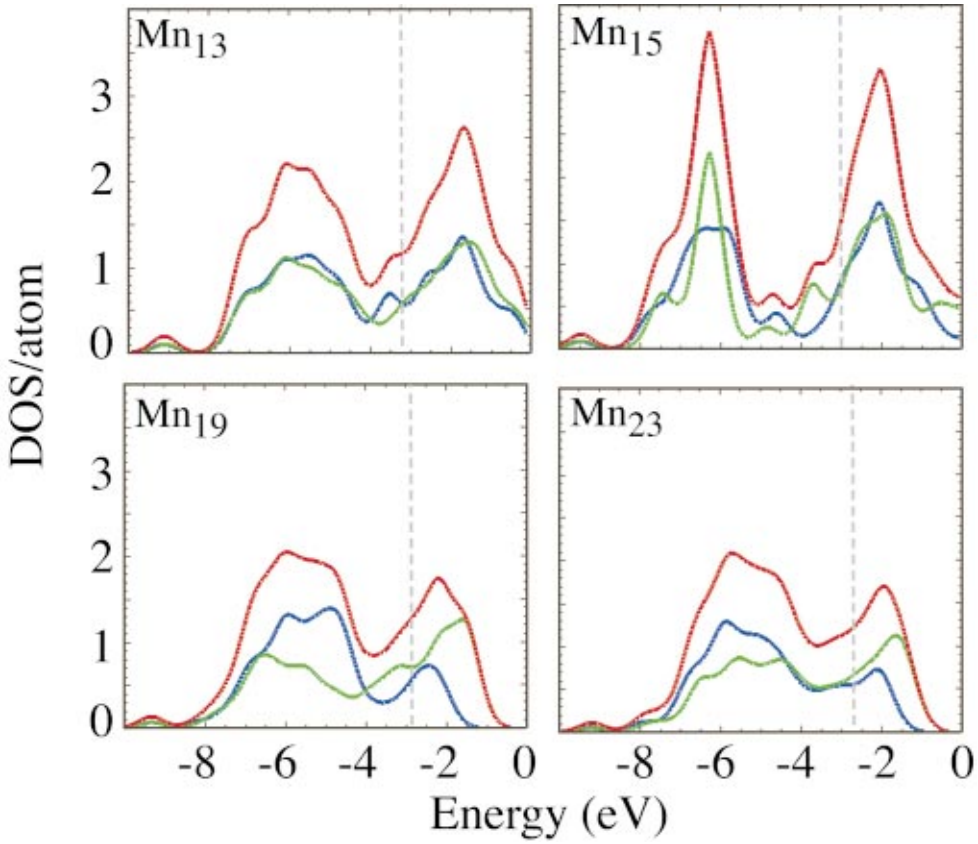

FIG. 2. (Color) Gaussian-broadened (half-width = 0.1 eV) densities of states for the lowest energy clusters. The spin up, spin down, and total density of states per atom are represented by the blue, green, and red lines, respectively. The gray vertical dashed lines indicate the Fermi energies.

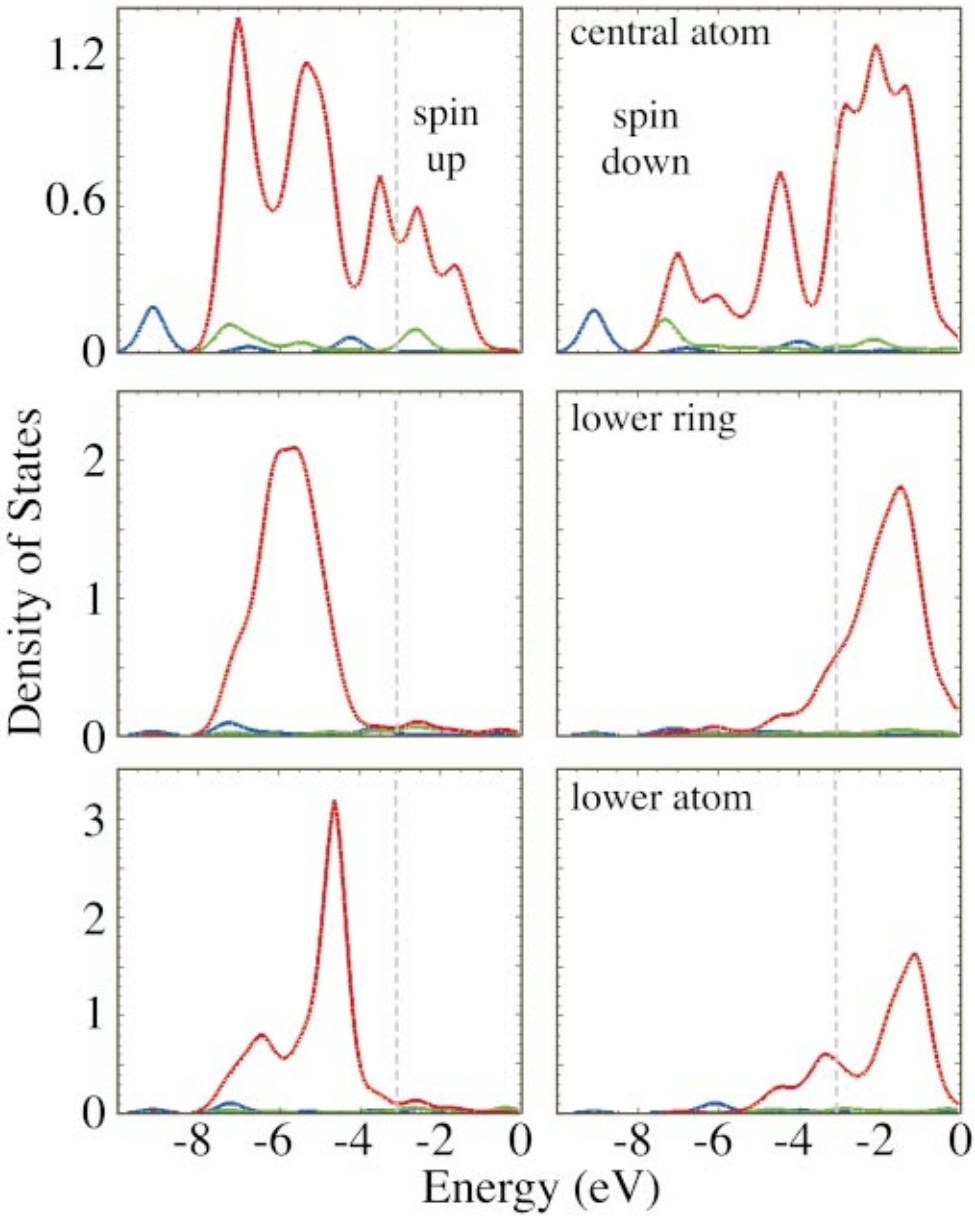

FIG. 3. (Color) Gaussian-broadened (half-width = 0.1 eV) partial densities of states for three representative atoms in the lowest energy Mn_{13} cluster. The *s*, *p*, and *d* partial densities are represented by the blue, green, and red lines, respectively. The grey vertical dashed lines indicate the Fermi energy.

relatively large moments on the lower ring and lower atoms (4.2 and $3.7\mu_B$, respectively). On the other hand, the *d*-projected LDOS for the central atom is rather broad for both the majority and minority spin states. The broadening occurs due to the high coordination of the central atom, and reflects the tendency towards metallic behavior. This tendency is also seen in the shorter bond lengths and smaller magnetic moment ($2.17\mu_B$). The beginning of metallic behavior is also seen from the small gaps between the highest occupied and lowest unoccupied molecular orbitals (HOMO-LUMO) gaps for all of the clusters, which range from 0.09 to 0.16 eV for the ground state structures.

The energies of the low lying isomers as a function of the magnetic moment relative to the ground state are shown in Fig. 4. Most of the lowest energy configurations are clustered near the minima, and there are several spin isomers lying close in energy. The general trend is towards lower net magnetic moments for Mn_{13} and Mn_{15} and higher net moments for Mn_{19} and Mn_{23}. More than one energy is shown for some moments, which is due to different spin configurations having the same total spin. This points to the delicacy of calculations in systems having antiferromagnetic coupling between spins on different atoms, where there is a drastic increase in the number of potential spin configurations for any net magnetic moment. It is found that more ordered spin arrangements are favored over the less ordered ones. Many of the less ordered icosahedral structures we explored have large ferromagnetic domains that are antiferromagnetically coupled to smaller domains. The interplay between domain size, degree of antiferromagnetic coupling, and symmetry appear to be maximized for the lowest energy structures. The second lowest energy structures for both Mn_{19} and Mn_{23} have the same basic spin arrangements as the ground state, but slightly different moments per atom. This demonstrates the stability of the ferromagnetic coupling within the rings and antiferromagnetic coupling between them.

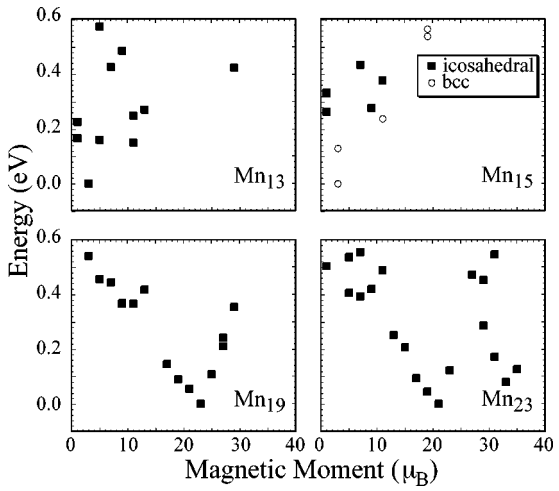

FIG. 4. Energy as a function of magnetic moment for each cluster size. For the 13-, 19-, and 23-atom clusters, only the icosahedral structures are included, whereas the energies of the low lying bcc isomers are also shown for Mn_{15}.

Interestingly, the second lowest energy configuration for Mn_{15} is also bcc, but with slightly shorter bond lengths, lower moments on the central and corner atoms, and higher moments on the face-centered atoms. This illustrates the challenge in dealing with such complicated systems, in that it is difficult to absolutely guarantee that we have reached the true minima in our calculations. However, a large sampling as well as the occurrence of ordered spin configurations that are of lowest energy lend support to our results.

In spite of the small energy differences between spin isomers, the temperature dependence of the net magnetic moment is expected to be rather weak, and only the lowest energy isomer will dominantly contribute at the temperature of 68 K used by Knickelbein.[6] A similar weak temperature dependence was obtained for Pd_{13}, which has a ferromagnetic ground state and much lower local moments.[14] Several closely lying spin configurations were also found for icosahedral Pd_{55} (Ref. 15) around the ground state, similar to what we have obtained for Mn_{19} and Mn_{23}.

The net theoretical and experimental moments are listed in Table I. The theoretical values of the net moments vary from 0.20 to $1.21\mu_B$/atom, while the experimental values range from 0.43 to $1.40\mu_B$/atom; however, the latter have large uncertainties. Based on this comparison, the theoretical finding of ferrimagnetic coupling resulting in small net moments is supported by experiment. The trend, however, is in disagreement with the experimental results. Although the theoretical moments for Mn_{13} and Mn_{23} are relatively close to experiment, Mn_{15} and Mn_{19} disagree. In the latter two cases, the theoretical magnetic moments respectively represent a local minimum and maximum, but experimentally the opposite holds. Because there are so many spin configurations close in energy, we cannot rule out the possibility that we have not found the lowest energy spin configuration for each cluster, or that another structural isomer is the true global minimum. Moreover, due to the icosahedral growth for smaller clusters, it is possible that bcc clusters are not favored in actual experimental growth conditions. The net moment per atom for Mn_{15} would then increase to $0.60\mu_B$, but this is still smaller than the experimental value of $1.40\mu_B$. There is a consistency in the theoretical spin configurations, however, in that the larger-sized icosahedral clusters naturally follow the pattern initiated with Mn_{13}. Another possible explanation for the discrepancy between theory and experiment is that noncollinear spin effects may be important, as has been shown for small chromium clusters.[16] This should be considered in future calculations. Also, the assumption in the Stern-Gerlach experiment was for ferromagnetically aligned superparamagnetic clusters.[6] Since this is not the case, we must consider if the experimental data should be reinterpreted for ferrimagnetic behavior.

In conclusion, we have studied the geometric and magnetic properties of Mn clusters with 13, 15, 19, and 23 atoms. Icosahedral structures are favored for Mn_{13} and Mn_{19}, while the bcc structure is favored for Mn_{15}. The magnetic behavior of the clusters is ferrimagnetic, and the spin configurations are quite well ordered. The clusters were shown to exhibit magnetic ordering that is qualitatively different from that seen in the antiferromagnetic bulk and smaller ferromagnetic clusters in that there are well-defined ferromagnetic domains of a few atoms that are antiferromagnetically coupled together. Our results confirm the low net moments per atom seen in experiment. An interesting finding is the competition between structural and spin ordering, as seen in Mn_{15}. This could lead to different structures for some Mn clusters that may not follow icosahedral growth due to the lack of higher symmetry spin alignment. This aspect of magnetic clusters should be further explored.

This work was partially supported by a Grant-In-Aid (No. 13750608) from the Japan Society for the Promotion of Science. The authors would like to thank the staff of the Center for Computational Materials Science at the Institute for Materials Research for computational assistance. We are also grateful for helpful discussions with Dr. Qiang Sun. V.K. thankfully acknowledges the kind hospitality of the Institute for Materials Research and the Center for Interdisciplinary Research of Tohoku University.

[1] V. Kumar, K. Esfarjani, and Y. Kawazoe, in *Clusters and Nanomaterials*, edited by Y. Kawazoe, T. Kondow, and K. Ohno, Springer Series in Cluster Physics (Springer-Verlag, Heidelberg, 2001), p. 9.

[2] A. Arrott and B. R. Coles, J. Appl. Phys. **32**, 51S (1961).

[3] M. R. Pederson, F. Reuse, and S. N. Khanna, Phys. Rev. B **58**, 5632 (1998).

[4] S. K. Nayak, B. K. Rao, and P. Jena, J. Phys.: Condens. Matter **10**, 10 863 (1998).

[5] N. Desmarais, F. A. Reuse, and S. N. Khanna, J. Chem. Phys.

112, 5576 (2000), and references therein.
[6] M. B. Knickelbein, Phys. Rev. Lett. **86**, 5255 (2001).
[7] G. Kresse and J. Furthmüller, Comput. Mater. Sci. **6**, 15 (1996); D. Vanderbilt, Phys. Rev. B **41**, 7892 (1990).
[8] J. P. Perdew and Y. Wang, Phys. Rev. B **45**, 13 244 (1992).
[9] We obtained a bond length of 2.60 Å and a binding energy of 0.325 eV/atom using the supercell method, which compares well with the earlier result of 2.61 Å and 0.315 eV/atom given in Ref. 5.
[10] The geometries of Mn_{13} and Mn_{19} were briefly reported in T. M. Briere, M. H. F. Sluiter, V. Kumar, and Y. Kawazoe, Mater. Trans., JIM **43**, 424 (2002).
[11] Q. Wang, Q. Sun, J.-Z. Yu, B.-L. Gu, Y. Kawazoe, and Y. Hashi, Phys. Rev. A **62**, 063203 (2000).
[12] V. Kumar and Y. Kawazoe, Phys. Rev. B **63**, 075410 (2001).
[13] S. K. Nayak, M. Noojien, and P. Jena, J. Phys. Chem. **103**, 9853 (1999).
[14] M. Moseler, H. Häkkinen, R. N. Barnett, and U. Landman, Phys. Rev. Lett. **86**, 2545 (2001).
[15] V. Kumar and Y. Kawazoe (unpublished).
[16] C. Kohl and G. F. Bertsch, Phys. Rev. B **60**, 4205 (1999).